

## On the Formation of the Trajectory of Propagation of Laser Radiation in the Anderson Differential Cell

© A.A. Goldberg,<sup>1</sup> R.V. Davydov,<sup>1</sup> I.D. Kochetkov,<sup>1</sup> V.V. Davydov,<sup>1,2</sup> D.S. Provodin<sup>1</sup>

<sup>1</sup>Peter the Great Saint-Petersburg Polytechnic University, St. Petersburg, Russia

<sup>2</sup>The Bonch-Bruевич Saint-Petersburg State University of Telecommunications,  
193232 Saint-Petersburg, Russia  
e-mail: davydov\_vadim66@mail.ru

Received September 14, 2022

Revised November 9, 2022

Accepted November 13, 2022

The necessity of studying the nature of the propagation of the maximum of the laser radiation pattern in the Anderson differential cell is substantiated. A new technique has been developed for conducting these studies, which takes into account all factors when constructing the trajectory of the maximum laser radiation in the cuvette, as well as outside it (up to the sensor of the photodiode line, on which the radiation is recorded). For the first time, an equation was derived to study the change in the nature of the propagation trajectory of the maximum of laser radiation in the Anderson cell, and beyond it, depending on its various parameters, the values of the refractive indices of the reference  $n_s$  and the liquid medium under study,  $n_m$ . The results of checking the reliability of the developed equation are presented. For the first time, a 12th degree polynomial was obtained for Anderson's differential cell with respect to the refractive index of the medium under study to obtain an analytical solution of the developed equation. This solution will provide additional information about the physics of the processes under consideration and the relationships between different quantities.

**Keywords:** laser radiation, refraction, liquid, refractive index, Anderson cell, spread trajectory, equation, polynomial.

DOI: 10.21883/TP.2023.01.55447.223-22

### Introduction

Currently, a special attention is paid to the development of fast and reliable methods of express testing of the state of condensed media [1–4]. It is connected to different causes, the main of which are environmental degradation, failure to meet conditions of storage and transportation of condensed media due to cost saving, as well as quality impairment in the production of media themselves, etc. [5–8]. Therefore, prior to the use of condensed media, especially when performing various experiments, the media need to be tested quickly to ensure reliability of the obtained results. This has resulted in a situation, that in addition to high requirements for accuracy and speed of measurement, as well as for the possibility to test large numbers of media, one more requirement has been added for the express test methods: measurements performed to determine the medium state must not change its physical structure and chemical composition [4,9–11]. The measurement of refractive index  $n_m$  of a condensed medium using the refraction phenomenon is one of options to solve the problem of express testing, that ensures meeting these requirements both in laboratory conditions and out of laboratories.

Scientific and technological advances have given rise to a large number of liquid media and their mixtures with

high refractive index  $n_m$  (for example, iodous methylene (diiodomethane) with  $n_m = 1.7425$  or solution of selenium and diarsenic disulfide in arsenic tribromide in a ratio of 1:1:3 with  $n_m = 2.1128$ , etc.). In this context the need has arisen to carry out additional research activities to search for new solutions to provide measurements of  $n_m$  in a large range of its variation with high accuracy. Previously performed studies [12–14] have shown, that one of possible options to solve this problem is related to the use of differential method of  $n_m$  measurement (differential refractometer with Anderson cuvette).

The analysis of results of different studies [15–20], as well as operation principles of differential refractometer designs [12–14] has shown, that in the consideration of Anderson cuvette two approximations were used that considerably limit accuracy and range of  $n_m$  measurement.

The first approximation. The laser beam passage through the Anderson cuvette was considered with an assumption that the partition thickness  $d$  (Fig. 1) between its two bays is an infinitely small value in comparison with geometrical dimensions of the cuvette ( $l_1$  — base length,  $l_2$  — base width). In these studies cuvettes were used with  $l_1 = 100–200$  mm,  $l_2 = 150–300$  mm at  $d = 0.5$  mm. Material was quartz glass ( $\alpha$ -quartz). Therefore, in the

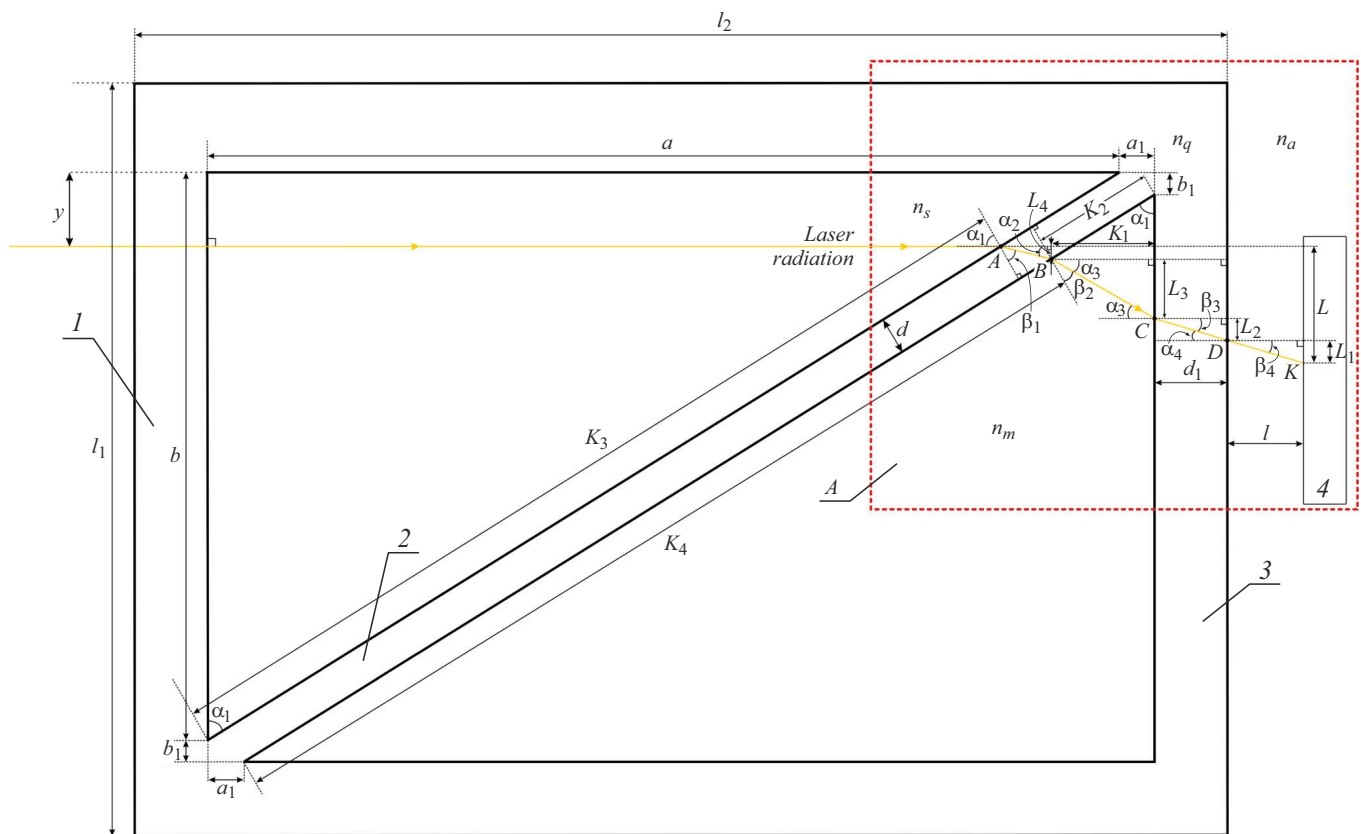


**Figure 1.** Anderson differential cuvette with direction of the maximum laser beam propagation: 1 — side face of the Anderson cuvette, on which the laser beam is incident; 2 — partition; 3 — side face of the Anderson cuvette, through which the laser beam leaves the cuvette; 4 — linear photodiode array.

relationship derived for the angle  $\varphi$  (this relationship is used to determine  $n_m$ ) of laser beam output from the Anderson cuvette after all refractions a certain error was included initially. This error increases at least three-four times with decrease in  $l_1$  and  $l_2$  of the cuvette. Currently, cuvettes with dimensions of  $l_1 = 30\text{--}50$  mm,  $l_2 = 40\text{--}100$  mm are commercially available for research purposes. This resulted in an increase in the error of  $n_m$  measurement and made low-demanded these refractometric measurements to test the state of biological and aqueous solutions of salts, medical suspensions, acids, alkalis, etc .

The second approximation. The relationship for the angle  $\varphi$ , which is used to determine  $n_m$ , was derived for a special case of Anderson cuvette ( $l_1 = l_2$ ). If the equation between faces  $l_1$  and  $l_2$  in the relationship for angle  $\varphi$  is not fulfilled, it was suggested to use a correction coefficient. Numerical values of this coefficient were supported by experimental data of  $n_m$  measurements with the use of differential refractometers. In these measurements of  $n_m$  the relationships were used, where a large error was included due to the absence of parameters of the cuvette partition. Therefore, a number of researchers in their works note that the use of this

coefficient may increase the measurement error of  $n_m$  up to 5% and over, which makes these measurements non-demanded. Therefore, they recommend to use for research purposes the Anderson differential cuvette with  $l_1 = l_2$  [15,17,18,21].

Our studies for the case of  $l_1 = l_2 \leq 60$  mm have shown that maximum laser beam at a large change in  $n_m$  may be out of the side face 3 of the Anderson cuvette (Fig. 1), which results in failure of the refractometer functioning. In the case of laser beam hitting a corner of the cuvette, it will be extremely difficult to measure  $n_m$ .

Therefore, the goal of this work is to derive an equation for investigation of features of the pattern of changes in the propagation of laser beam axis trajectory without approximations both in the Anderson cuvette and out of the cuvette upstream of the photosensitive sensor of the linear photodiode array where the radiation is recorded, depending on cuvette parameters, values of refractive index of the reference liquid  $n_s$  and liquid to be measured  $n_m$ , as well as distance  $l$  (Fig. 1). This will allow ensuring high accuracy of  $n_m$  measurement in a wide range of its changes.

## 1. Formation of the trajectory of laser beam maximum propagation in the Anderson differential cuvette and its features

Fig. 1 shows scheme of the Anderson differential cuvette with the direction of laser beam axis trajectory propagation from the outer cuvette wall  $I$  to the photo-sensitive sensor on the linear photodiode array  $4$ . The use of linear photodiode array to record laser beam in refractometers is the most reasonable option currently [13,14,16,18,22,23].

The structure of laser beam axis trajectory formation from the wall  $I$  to the sensor  $4$  is based on the radiation refraction at the boundary of several media with different refractive indices in points  $A, B, C$ , and  $D$  (Fig. 1). We consider vertical shifts of points  $B, C, D$ , and  $K$  (parallel to face  $I$ ) in relation to point  $A$  (Fig. 1). For each shift (distances  $L_1, L_2, L_3$ , and  $L_4$ ) a mathematical relationship is derived taking into account cuvette parameters (geometrical dimensions, material, etc.), refractive indices  $n_s$  and  $n_m$ , places of laser beam enter into the cuvette (face  $I$  — point  $O$  — distance  $y$ ) and distance  $l$  to the linear photodiode array  $4$ .

Our studies have shown that in the consideration of laser beam axis trajectory a number of features arise, the main of which is related to the taking into account parameters of the partition 2 (Fig. 1), i.e. the value of  $d$  and refractive index  $n$  of the partition material, in the equation that describes the laser beam axis trajectory. Usually, three materials are used for the partition: quartz, sapphire, and KV glass. It is worth to note that the same material is used to manufacture other faces of the Anderson cuvette. In this case it is necessary to consider three variants of trajectory formation. These variants are connected to the ratio between the refractive index  $n_m$  and, for example,  $n_q$  (the cuvette is made of quartz). Three situations are possible in the process of studying ( $n_m > n_q$ ,  $n_m = n_q$ , and  $n_m < n_q$ ). In this case one more feature needs to be taken into consideration, which is related to the ratio between  $n_s$  and  $n_q$ . If  $n_s > n_q$ , a complete internal reflection can take place at the interface of two media. Previously it was not taken into consideration in the measurement of angle  $\varphi$  to determine  $n_m$ . Some researchers assumed the possibility of such situation, therefore, to conduct studies, it was recommended to use a reference liquid with  $n_s < n_q$ . The studies carried out by the authors of this work have shown that to improve accuracy of  $n_m$  measurement, it may be necessary to use a reference liquid with  $n_s > n_q$ . In this case it is necessary to exclude fulfilment of the following relationship, corresponding to complete internal reflection at the interface of two media:

$$\frac{n_s}{n_q} \sin(\alpha_1) > 1. \quad (1)$$

Results of the studies have shown that to fulfil relationship (1) for the reference liquids used in real conditions for the measurement, it is necessary to have angle  $\alpha_1$  (Fig. 1) greater than  $60^\circ$ . Therefore, dimensions of the Anderson cuvette should be selected to ensure fulfilment of the above-mentioned condition. To perform exclusive studies, for example, with  $n_s > 1.7$ , special cuvettes with  $\alpha_1 = 30^\circ$  are used, which excludes fulfilment of relationship (1).

Let us now consider the situations related to the fact that it is difficult to prognose value of  $n_m$  since it can vary due to different reasons. In addition, value of  $n_m$  must be measured with a high accuracy (at least  $10^{-3}$ ). The first situation is connected to the relationship of  $n_m > n_q$ . In this case the trajectory of laser beam axis change is shown in Fig. 1. The second situation is when  $n_m = n_q$ . Our experiments have shown that to describe the change in trajectory of the laser beam axis in this case, the equation can be used that was derived for the case of  $n_m > n_q$ . The third situation (connected to the relationship of  $n_m < n_q$ ) for a differential refractometer is considered for the first time. In this case the refracted laser beam (Fig. 1, point  $B$ ) propagates above the straight line  $OA$ . This situation is also taken into account in this work, because the derivation of the mathematical relationship to determine  $L = L_1 + L_2 + L_3 + L_4$  takes into account the presence of partition in the cuvette with parameters  $d$  and  $n_q$ . The use of previously derived relationships without taking into account these parameters to determine  $n_m$  when carrying out measurement by previously developed refractometers resulted in large errors.

Fig. 2 shows fragment  $A$  from Fig. 1 for a more clear representation of the derivation of relationships to determine  $L_1, L_2, L_3$ , and  $L_4$  when considering the change in trajectory of the laser beam axis for the case of  $n_m > n_q$ .

When considering the third situation ( $n_m < n_q$ ), one more feature should be taken into account, which is related to the phenomenon of complete internal reflection of laser beam at the interface of two media when the radiation propagates from a medium with higher density to a medium with lower density ( $n_q > n_m$ ). For this case, it is necessary to define the condition of complete internal reflection and develop methods that make it possible to exclude the effect of this factor on the measurement of  $n_m$ .

Let us consider the change in the laser beam axis trajectory shown in Fig. 2. The complete internal reflection at the interface of two media (quartz and the medium under study) takes place when the following relationship is fulfilled:

$$\sin(\beta_2) \frac{n_q}{n_m} = \sin(\alpha_2) > 1. \quad (2)$$

Taking into account the fact that upstream of this interface the laser beam is refracted one more time at the interface of two media with  $n_s$  and  $n_q$ , relationship (2) can be

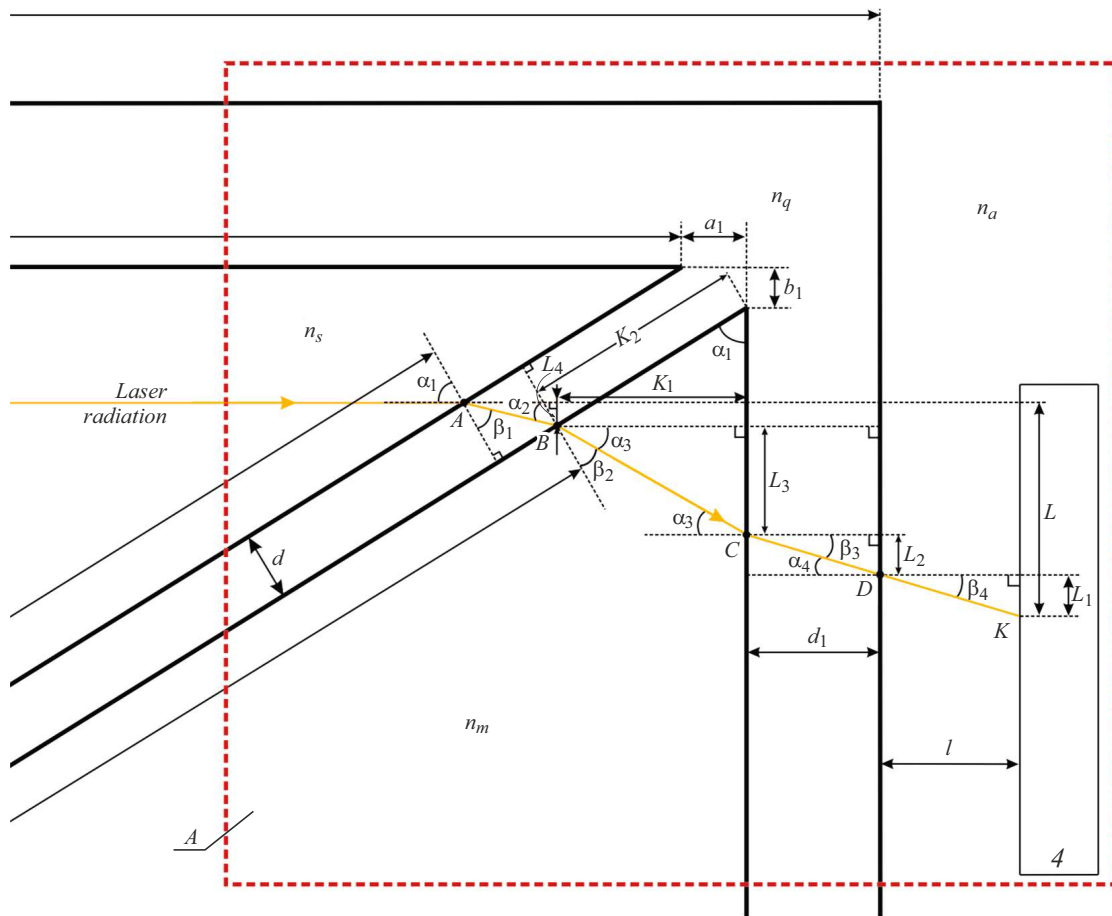


Figure 2. Fragment A — Anderson differential cuvette with a linear photodiode array.

transformed as follows:

$$\frac{n_s}{n_m} \sin(\alpha_1) > 1. \tag{3}$$

The resulted relationship (3) shows that the complete internal reflection of laser beam at the above-mentioned interface of two media takes place only in the case of  $n_s > n_m$  for certain angles  $\alpha_1$  that depend on geometrical dimensions of the cuvette. Previously, in the consideration of relationship (1) it was found that  $\alpha_1 < 60^\circ$ . In this case the complete internal reflection at the interface of two media takes place when the following relationship is fulfilled:

$$\frac{n_s}{n_m} \geq 1.155. \tag{4}$$

For  $\alpha_1 = 45^\circ$ , relationship (3) can be transformed as follows:

$$\frac{n_s}{n_m} \geq 1.414. \tag{5}$$

The experience of differential refractometers operation shows that fulfilment of condition (4) can only possible in the process of studies in the case of solving special problems. In this situation it is recommended to use an Anderson cuvette with  $\alpha_1 = 30^\circ$  or less, since in this case

the probability of fulfilment of (5) is close to zero. It is necessary to note, that relationships (4) and (5) with a high probability can be fulfilled, if the reference liquid and the liquid under study are confused with each other in the process of studies (the liquids are poured in wrong bays of the Anderson differential cuvette). In this case the directional pattern on the linear photodiode array 4 will have no signal of the laser beam with a clearly defined maximum. Reliable measurements of  $n_m$  will be impossible, since photosensitive sensors of the linear photodiode array will be exposed to multiple-reflected weak signals of the laser beam. To prevent unreliable measurements of  $n_m$  based on these signals, the following is implemented in the processing of signals from the linear photodiode array. The output signal  $U$  from the linear photodiode array 4 is normalized according to the following principle:

$$U = \frac{\sum_{i=1}^{1024} U_i}{U_{\max}}, \tag{6}$$

where  $U_{\max}$  — maximum illumination signal from an element of the linear photodiode array,  $U_i$  — amplitude of the signal from an element of photodiode cell,  $i$  — number

of the element. This allows unambiguous identification of the presence of one clearly defined maximum on sensors of the linear photodiode array from the laser beam passed through several media in the Anderson cuvette. If multiple-reflected optical signals arrive at the linear photodiode array, little bursts of  $U$  amplitude are clearly identified, which are unambiguously different from a clearly defined maximum. Previously, in the methods used to process optical signals in differential refractometers this was not implemented.

In addition, the use of this technique allows unambiguous identification of axis position of the laser beam to be recorded (amplitude maximum) when the beam shape is distorted due to absorption of the laser beam and subsequent its emission in the medium under study (the reference liquid is selected such that these process are minimized), as well as identification of light bursts or distortions in the laser beam shape (for unambiguous identification of axis position of the laser beam) due to the scattering when investigating a medium where another medium is added, and a small part is remained undissolved. A similar situation can take place when tasting the state of hydrocarbon media, where one medium in a small quantity has entered into another medium (for example, alcohols, aviation kerosene, etc.). This technique can be effectively used in the case of formation of minor speckles. Distortions of the beam shape are small, and axis position of the laser beam on sensors of the linear photodiode array can be determined.

In the case of presence of different particles in the medium under study that cause scattering of the laser beam, for example, Mie scattering, the distortions of the laser beam shape will be significant, and it will be extremely difficult to determine axis position of the laser beam on the linear photodiode array.

If speckles are formed due to some reasons, for example, undissolved impurities (in minor concentrations) with a size of about 0.02 and over of the laser beam width, it will be impossible to identify axis position of the laser beam on the linear photodiode array. It is necessary to note that this issue needs additional extensive studying with specially produced model media.

Therefore, prior to derive an equation for description of the change in axis position of the laser beam when it passes through a differential cuvette with liquid media and the distance to the linear photodiode array, let us define the following. The geometrical-beam approach for description of the change of laser beam axis is considered by us when liquid media are transparent, homogeneous, distortions in the wave front are minimal. Various difficulties in the identification of axis position of the laser beam when recording it at a linear photodiode array were considered earlier.

## 2. Equation for description of the laser beam axis change

As an example, let us present the derivation of an equation to describe the change in laser beam axis for the situation of  $n_m > n_q$ . Let us consider fragment A (Fig. 2) and write the following relationships:

$$A : \frac{\sin \alpha_1}{\sin \beta_1} = \frac{n_q}{n_s}; \quad B : \frac{\sin \alpha_2}{\sin \beta_2} = \frac{n_m}{n_q}; \quad C : \frac{\sin \alpha_3}{\sin \beta_3} = \frac{n_q}{n_m};$$

$$D : \frac{\sin \alpha_4}{\sin \beta_4} = \frac{n_a}{n_q};$$

$$\alpha_1 = \alpha_3 + \beta_2, \quad L_1 = l \operatorname{tg} \beta_4, \quad L_2 = d_1 \operatorname{tg} \beta_3, \quad L_3 = K_1 \operatorname{tg} \alpha_3,$$

$$K_1 = (y - b_1 + L_4) \operatorname{tg} \alpha_1, \quad \operatorname{tg} \alpha_1 = \frac{a}{b},$$

$$L_4 = |AB| \sin(\alpha_1 - \beta_1) = \frac{d}{\cos \beta_1} \sin(\alpha_1 - \beta_1)$$

$$= d(\sin \alpha_1 - \cos \alpha_1 \operatorname{tg} \beta_1),$$

$$\frac{\sin \alpha_1}{\sin \beta_1} = \frac{n_q}{n_s} \Rightarrow \sin \beta_1 = \frac{n_s}{n_q} \sin \alpha_1,$$

$$\operatorname{tg} \beta_1 = \frac{n_s \sin \alpha_1}{\sqrt{n_q^2 - n_s^2 \sin^2 \alpha_1}}.$$

These relationships then allow for expression of  $L_1, L_2, L_3$ , and  $L_4$  through Anderson cuvette parameters, distance  $l$ , as well as refractive indices of the reference liquid  $n_s$  and the liquid medium under study  $n_m$ .

$$L_4 = d \sin \alpha_1 \left( 1 - \frac{n_s \cos \alpha_1}{\sqrt{n_q^2 - n_s^2 \sin^2 \alpha_1}} \right), \quad (7)$$

$$\operatorname{tg} \alpha_3 = \operatorname{tg}(\alpha_1 - \beta_2) = \frac{\operatorname{tg} \alpha_1 - \operatorname{tg} \beta_2}{1 + \operatorname{tg} \alpha_1 \operatorname{tg} \beta_2},$$

$$\frac{\sin \alpha_1}{\sin \beta_1} = \frac{n_q}{n_s}; \quad \frac{\sin \alpha_2}{\sin \alpha_2} = \frac{n_m}{n_q},$$

$$\alpha_2 = \beta_1 \Rightarrow \frac{\sin \alpha_1}{\sin \beta_2} = \frac{n_m}{n_s} \Rightarrow \sin \beta_2 = \frac{n_s}{n_m} \sin \alpha_1,$$

$$\operatorname{tg} \beta_2 = \frac{\frac{n_s}{n_m} \sin \alpha_1}{\sqrt{1 - \frac{n_s^2}{n_m^2} \sin^2 \alpha_1}} = \frac{n_s \sin \alpha_1}{\sqrt{n_m^2 - n_s^2 \sin^2 \alpha_1}},$$

$$\begin{aligned} \frac{L_3}{K_1} = \operatorname{tg} \alpha_3 &= \frac{\operatorname{tg} \alpha_1 - \frac{n_s \sin \alpha_1}{\sqrt{n_m^2 - n_s^2 \sin^2 \alpha_1}}}{1 + \operatorname{tg} \alpha_1 \frac{n_s \sin \alpha_1}{\sqrt{n_m^2 - n_s^2 \sin^2 \alpha_1}}} \\ &= \frac{\sin \alpha_1 \sqrt{n_m^2 - n_s^2 \sin^2 \alpha_1} - n_s \sin \alpha_1 \cos \alpha_1}{\cos \alpha_1 \sqrt{n_m^2 - n_s^2 \sin^2 \alpha_1} + n_s \sin^2 \alpha_1}, \end{aligned}$$

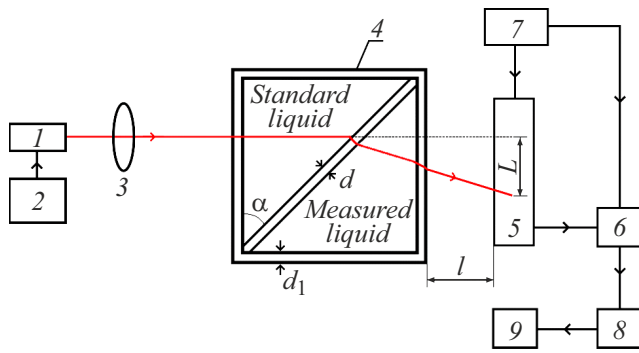


**Figure 3.** Structural diagram of the laboratory mockup of differential refractometer: 1 — semiconductor laser; 2 — power supply unit of the laser; 3 — lens; 4 — Anderson cuvette; 5 — linear photodiode array; 6 — analog-to-digital converter; 7 — multifunctional power supply unit; 8 — processing device; 9 — laptop.

$$\frac{\sin \alpha_3}{\sin \beta_3} = \frac{n_q}{n_m} \Rightarrow \sin \beta_3 = \frac{n_m}{n_q} \sin \alpha_3 \Rightarrow \operatorname{tg} \beta_3 = \frac{\frac{n_m}{n_q} \sin \alpha_3}{\sqrt{1 - \frac{n_m^2}{n_q^2} \sin^2 \alpha_3}} = \frac{n_m \sin \alpha_3}{\sqrt{n_q^2 - n_m^2 \sin^2 \alpha_3}},$$

$$\begin{aligned} \sin \alpha_3 &= \sin(\alpha_1 - \beta_2) = \sin \alpha_1 \cos \beta_2 - \sin \beta_2 \cos \alpha_1 \\ &= \sin \alpha_1 \sqrt{1 - \frac{n_s^2}{n_m^2} \sin^2 \alpha_1} - \frac{n_s}{n_m} \sin \alpha_1 \cos \alpha_1 \\ &= \frac{\sin \alpha_1}{n_m} \left( \sqrt{n_m^2 - n_s^2 \sin^2 \alpha_1} - n_s \cos \alpha_1 \right), \end{aligned}$$

$$\operatorname{tg} \beta_3 = \frac{L_2}{d_1} = \frac{\sin \alpha_1 \left( \sqrt{n_m^2 - n_s^2 \sin^2 \alpha_1} - n_s \cos \alpha_1 \right)}{\sqrt{n_q^2 - \sin^2 \alpha_1 (n_m^2 + n_s^2 \cos^2 \alpha_1 - n_s^2 \sin^2 \alpha_1) - 2n_s \cos \alpha_1 \sqrt{n_m^2 - n_s^2 \sin^2 \alpha_1}}},$$

$$L_1 = l \operatorname{tg} \beta_4, \quad \frac{\sin \alpha_3}{\sin \beta_3} = \frac{n_q}{n_m}; \quad \frac{\sin \alpha_4}{\sin \beta_4} = \frac{n_a}{n_q};$$

$$\alpha_4 = \beta_3 \Rightarrow \frac{\sin \alpha_3}{\sin \beta_4} = \frac{n_a}{n_m} \Rightarrow \sin \beta_4 = \frac{n_m}{n_a} \sin \alpha_3,$$

$$\begin{aligned} \sin \alpha_3 &= \frac{\sin \alpha_1}{n_m} \left( \sqrt{n_m^2 - n_s^2 \sin^2 \alpha_1} - n_s \cos \alpha_1 \right) \Rightarrow \sin \alpha_6 \\ &= \frac{\sin \alpha_1}{n_a} \left( \sqrt{n_m^2 - n_s^2 \sin^2 \alpha_1} - n_s \cos \alpha_1 \right), \end{aligned}$$

$$\begin{aligned} \frac{L_1}{l} = \operatorname{tg} \beta_4 &= \frac{\frac{\sin \alpha_1}{n_a} \left( \sqrt{n_m^2 - n_s^2 \sin^2 \alpha_1} - n_s \cos \alpha_1 \right)}{\sqrt{1 - \left( \frac{\sin \alpha_1}{n_a} \left( \sqrt{n_m^2 - n_s^2 \sin^2 \alpha_1} - n_s \cos \alpha_1 \right) \right)^2}} \\ &= \frac{\sin \alpha_1 \left( \sqrt{n_m^2 - n_s^2 \sin^2 \alpha_1} - n_s \cos \alpha_1 \right)}{\sqrt{n_a^2 - \sin^2 \alpha_1 (n_m^2 - n_s^2 \sin^2 \alpha_1 + n_s^2 \cos^2 \alpha_1) - 2n_s \cos \alpha_1 \sqrt{n_m^2 - n_s^2 \sin^2 \alpha_1}}}. \end{aligned}$$

This allowed us to obtain the following relationship for  $L$ :

$$\begin{aligned} L = L_1 + L_2 + L_3 + L_4 &= \sin \alpha_1 \left( d \left( 1 - \frac{n_s \cos \alpha_1}{\sqrt{n_q^2 - n_s^2 \sin^2 \alpha_1}} \right) \right. \\ &+ \left( \sqrt{n_m^2 - n_s^2 \sin^2 \alpha_1} - n_s \cos \alpha_1 \right) \\ &\times \left( \frac{l}{\sqrt{n_a^2 - \sin^2 \alpha_1 (n_m^2 - n_s^2 \sin^2 \alpha_1 + n_s^2 \cos^2 \alpha_1) - 2n_s \cos \alpha_1 \sqrt{n_m^2 - n_s^2 \sin^2 \alpha_1}}} \right. \\ &+ \frac{d_1}{\sqrt{n_q^2 - \sin^2 \alpha_1 (n_m^2 + n_s^2 \cos^2 \alpha_1 - n_s^2 \sin^2 \alpha_1) - 2n_s \cos \alpha_1 \sqrt{n_m^2 - n_s^2 \sin^2 \alpha_1}}} \\ &\left. \left. + \frac{K_1}{\cos \alpha_1 \sqrt{n_m^2 - n_s^2 \sin^2 \alpha_1 + n_s \sin^2 \alpha_1}} \right) \right). \end{aligned} \quad (8)$$

Relationship (8) was verified for reliability using the mockup of differential refractometer with Anderson cuvette developed by us (Fig. 3). In two sections of the Anderson cuvette liquid media with known refractive indices were accommodated. One of these medium served as the reference medium —  $n_s$ , another one was the medium to be measured —  $n_m$ . When placing the liquid media in sections of the Anderson cuvette, relationships (1), (3), (4), and (5) (that were used to derive relationship (8)) were taken into consideration. The laboratory mockup of differential refractometer makes use of a semiconductor laser 1 with built-in optical devices. The laser is custom-built by „Hamamatsu Photonics“ (Japan) for „ATAGO“ company (Japan).

Wavelength is  $\lambda = 632.8$  nm, power  $P$  of the laser beam is adjustable to 20 mW. Downstream of lens 3 the laser beam divergence angle is  $\theta \approx 0.02$  mrad. Lens 3 is a macrolens (of toric shape) and is located near the end of laser crystal (built-in optics). It transforms the wave front of laser beam into a plane-parallel front. The laser is operated with transversal fundamental mode. The adjustment of power  $P$  is necessary to investigate media with different transparency. From the semiconductor laser 1 (Fig. 3) the beam is incident on the side face 1 of the

**Table 1.** Shifts  $L$  of the laser beam maximum on the linear photodiode array for the case of  $n_s = n_m < n_q$  for a temperature of liquid media and quartz equal to  $T = 293.1$  K

Medium	$n_s = n_m$	$n_q$	$L_m$ , mm	$L_c$ , mm
Air	1.000273	1.537826	$1.4381 \pm 0.0005$	1.437762
Water	1.327412	1.537826	$0.0828 \pm 0.0005$	0.082450
Alcohol (ethyl)	1.361513	1.537826	$0.0715 \pm 0.0005$	0.071131
AI-92 gasoline	1.437762	1.537826	$0.0440 \pm 0.0005$	0.043715

**Table 2.** Shifts  $L$  of the laser beam maximum on the linear photodiode array for the case of  $n_s = n_m > n_q$  for a temperature of liquid media and quartz equal to  $T = 293.1$  K

Medium	$n_s = n_m$	$n_q$	$L_m$ , mm	$L_c$ , mm
Aniline	1.562442	1.537826	$0.0247 \pm 0.0005$	-0.024355
Carbon sulfide	1.623018	1.537826	$0.0409 \pm 0.0005$	-0.040534
Iodous methylene	1.742556	1.537826	$0.1168 \pm 0.0005$	-0.116417

Anderson cuvette (Fig. 1) at a right angle. To record the laser beam, a TSL1406RSM linear photodiode array (by AMS-TAOS USA) is used with 1024 photosensitive sensors, which is custom-built for „ATAGO“ company (Japan). Width of the recording zone is 64.6 mm, height of the zone is 3.6 mm. Size of the photosensitive sensor is  $(0.062 \times 1.6)$  mm. Distance between sensors along the length of the linear photodiode array is 0.001 mm. The error of determining distance  $L$  in this case is 0.0005 mm (half distance between photosensitive sensors — uncertainty of axis position (amplitude maximum) of the recorded laser beam).

This configuration of the laser beam recording allows controlling of the beam shape and investigating the evolution of the laser beam shape depending on the state of the medium under study even in cases when, due to the presence of speckles, it is impossible to determine the

position of laser beam axis on the linear photodiode array. These investigations then allow determining the functionality of the developed differential refractometer for studying of different media.

Width of the beam was measured at a level of 0.5 at a distance of 300 mm from the laser without the cuvette. The width is  $0.448 \pm 0.001$  mm. Then in the studying of liquid media, the laser beam width on sensors of the linear photodiode array increases depending on properties of the medium under study and the reference medium, as well as temperature  $T$  of them.

Table 1–3 shows results of comparison between measured  $L_m$  and calculated  $L_c$  values using (8) for different liquid media. The following parameters were used for the calculations:  $n_q = 1.537826$ ,  $n_a = 1.000273$ ,  $d = 0.5$  mm,  $d_1 = 1$  mm,  $l = 20$  mm,  $y = 4$  mm.

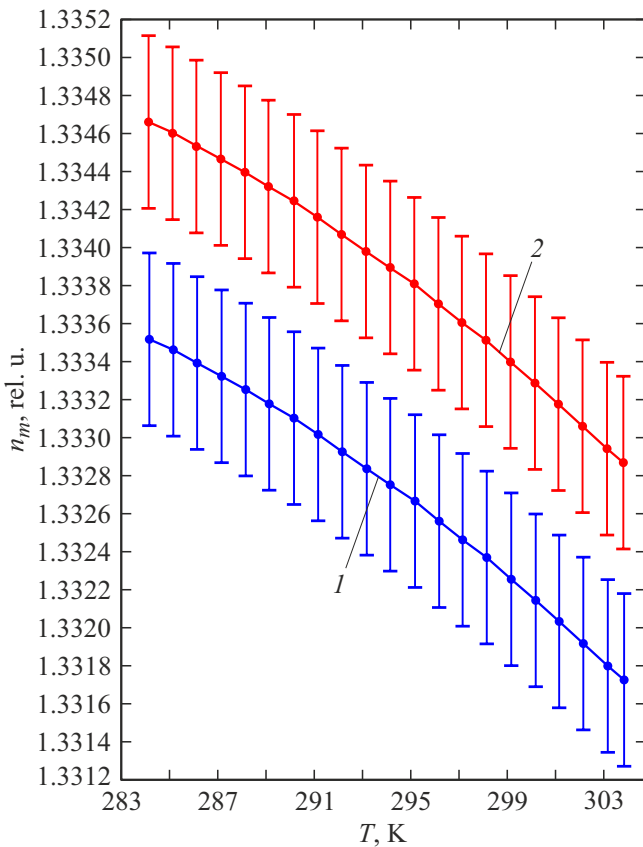
The analysis of obtained results has shown that  $L_m$  and  $L_c$  coincide with each other within the measurement accuracy of  $L_m$ , which confirm the reliability of relationship (8) derived by us and the possibility of its use in the developed differential refractometer (Fig. 3) to determine  $n_m$ .

Fig. 4 shows, as an example of functionality verification of the developed differential refractometer, the results of investigation of the state of the tap water and the aqueous solution with oxides, which is used in biological experiments, at different temperatures  $T$ . The aqueous solution with oxides was prepared from the tap water and 10% aqueous solution of nitric acid (in a ratio of 97 to 3 by volume). The state of water and solution is determined by the measured value of  $n_m$  using (8). The obtained results match the data of studies carried out by other researchers [13,15,18,19,20,22–24].

To additionally confirm the reliability of results of  $n_m$  measurement obtained with the use of the developed refractometer design and relationship (8), we investigated the measurements of refractive index of Rheinol 5W-30 engine oil as a function of temperature  $T$  and compared these results with the data obtained with the help of commercial Abbe NAR-2T refractometer (by „ATAGO“, Japan) with a measurement error of 0.0002. Table 4 presents results of comparison between refractive indices measured using two instruments.

**Table 3.** Shifts  $L$  of the laser beam maximum on the linear photodiode array for the case of  $n_s < n_q$ , any values of  $n_m$  for a temperature of liquid media and quartz equal to  $T = 293.1$  K

Reference medium	$n_s$	Medium to be measured	$n_m$	$n_q$	$L_m$ , mm	$L_c$ , mm
Air	1.000273	Alcohol (ethyl)	1.361513	1.537826	$0.7708 \pm 0.0005$	0.770416
Water	1.327412	AI-92 gasoline	1.437762	1.537826	$2.4711 \pm 0.0005$	2.470831
Alcohol (ethyl)	1.361513	Carbon sulfide	1.623018	1.537826	$6.4642 \pm 0.0005$	6.463831
AI-92 gasoline	1.437762	Iodous methylene	1.742556	1.537826	$9.1239 \pm 0.0005$	9.123527



**Figure 4.** Dependence of change in refractive index  $n_m$  of the tap water on temperature  $T$ . The graph correspond to the following state of tap water: 1 — no oxides in the water, 2 — there are oxides in the water.

The analysis of data presented in Table 4 shows, that results of  $n_m$  measurement are consisted within the measurement accuracy, which confirms reliability of relationship (8) derived by us and justification of the suggested technique of  $n_m$  measurement using Anderson differential cuvette.

Then, to derive an analytical relationship for  $n_m(d, L, n_s, l, d_1, n_q, \alpha_1)$ , let us introduce the following denominations:

$$\frac{L_4}{\sin \alpha_1} = d \left( 1 - \frac{n_s \cos \alpha_1}{\sqrt{n_q^2 - n_s^2 \sin^2 \alpha_1}} \right) = L'_4,$$

$$\frac{L}{\sin \alpha_1} - L'_4 = \frac{L - L_4}{\sin \alpha_1} = A,$$

$$\sqrt{n_m^2 - n_s^2 \sin^2 \alpha_1} - n_s \cos \alpha_1 = f_1,$$

$$f_1^2 = n_m^2 - n_s^2 \sin^2 \alpha_1 + n_s^2 \cos^2 \alpha_1 - 2n_s \cos \alpha_1 \sqrt{n_m^2 - n_s^2 \sin^2 \alpha_1},$$

$$f_2^2 = f_1^2 \sin^2 \alpha_1, \quad f_2 = f_1 \sin \alpha_1,$$

**Table 4.** Change in refractive index  $n_m$  of engine oil as a function of temperature  $T$

$T$ , K	Laboratory mockup of differential refractometer	Commercial refractometer Abbe NAR-2T
$285.1 \pm 0.1$	$1.4707 \pm 0.0005$	$1.4703 \pm 0.0002$
$287.2 \pm 0.1$	$1.4701 \pm 0.0005$	$1.4699 \pm 0.0002$
$291.3 \pm 0.1$	$1.4685 \pm 0.0005$	$1.4682 \pm 0.0002$
$295.2 \pm 0.1$	$1.4669 \pm 0.0005$	$1.4665 \pm 0.0002$
$299.3 \pm 0.1$	$1.4654 \pm 0.0005$	$1.4650 \pm 0.0002$
$303.2 \pm 0.1$	$1.4640 \pm 0.0005$	$1.4637 \pm 0.0002$
$307.2 \pm 0.1$	$1.4625 \pm 0.0005$	$1.4621 \pm 0.0002$
$310.1 \pm 0.1$	$1.4611 \pm 0.0005$	$1.4607 \pm 0.0002$
$313.2 \pm 0.1$	$1.4596 \pm 0.0005$	$1.4591 \pm 0.0002$

$$A = f_1 \left( \frac{l}{\sqrt{n_a^2 - f_2^2}} + \frac{d_1}{\sqrt{n_q^2 - f_2^2}} + \frac{K_1}{\cos \alpha_1 (f_1 + n_s \cos \alpha_1) + n_s \sin^2 \alpha_1} \right),$$

$$\frac{A}{f_1} = \frac{l}{\sqrt{n_a^2 - f_2^2}} + \frac{d_1}{\sqrt{n_q^2 - f_2^2}} + \frac{K_1}{f_1 \cos \alpha_1 + n_s}.$$

In this case, equation (8) is transformed to the following form:

$$\frac{A \sin \alpha_1}{f_2} = \frac{l}{\sqrt{n_a^2 - f_2^2}} + \frac{d_1}{\sqrt{n_q^2 - f_2^2}} + \frac{K_1}{f_2 \operatorname{tg} \alpha_1 + n_s}$$

$$\frac{L_0}{f_2} - \frac{K_1}{f_2 \operatorname{tg} \alpha_1 + n_s} = \frac{l}{\sqrt{n_a^2 - f_2^2}} + \frac{d_1}{\sqrt{n_q^2 - f_2^2}}. \quad (9)$$

In the resulted relationship (9) the unknown  $n_m$ , which needs to be determined as a result of measurement of  $L$ , is only presented in one variable  $f_2(n_m)$ . Equation (9) can be only solved numerically for  $n_m$ . Therefore, to obtain an analytical relationship for  $n_m(d, L, n_s, l, d_1, n_q, \alpha_1)$ , we transform (9). As a result of performed transformations we get relationship (10), which is a polynomial of degree 12 in  $f_2$ . Roots of this polynomial are explicit relationships for  $n_m$  in relation to variables  $d, L, n_s, l, d_1, n_q$  and  $\alpha_1$ . Relationship (10) takes into account all factors affecting the formation of trajectory of the laser beam axis in the Anderson differential cuvette and out of it to the linear photodiode array 4 (Fig. 2).

Based on the experimental values of  $n_m$  obtained on the laboratory mockup using (8), we verified the derivation of equation (10), for which purpose we substituted all values

into equation (10) and obtained zero. This is an achievement of the approach proposed by us, that allows finding an error in mathematical transformations and derivations, which is absent in a number of works related to solving of theoretical problems.

Currently, method are developed that allows finding a general solution to a fourth-degree equation. In general, coefficients of our polynomial are real numbers, therefore, to find its roots we essentially can use only one method: factorial expansion. Therefore, we plan to factorize the polynomial using the supercomputer of the Peter the Great St.Petersburg Polytechnic University.

$$\begin{aligned}
 P(f_2) = & f_2^{12}(C^4 + e^4 \operatorname{ctg}^4(\alpha_1) + d_1^4 \operatorname{ctg}^4(\alpha_1) - 2e^2 d_1^2 \operatorname{ctg}^4(\alpha_1) \\
 & + 2(e^2 + d_1^2)C^2 \operatorname{ctg}^2(\alpha_1)) + f_2^{11}(4C^3 B + 4e^4 n_s \operatorname{ctg}^3(\alpha_1) \\
 & + 4d_1^4 n_s \operatorname{ctg}^3(\alpha_1) - 8e^2 d_1^2 n_s \operatorname{ctg}^3(\alpha_1) + 4(e^2 + d_1^2)C \operatorname{ctg}(\alpha_1) \\
 & \times (n_s C + \operatorname{ctg}(\alpha_1)B)) + f_2^{10}(-C^4(2n_a^2 + 2n_q^2) + 6C^2 B^2 \\
 & - 2n_q^2 e^4 \operatorname{ctg}^4(\alpha_1) + 6e^4 n_s^2 \operatorname{ctg}^2(\alpha_1) - 2n_a^2 d_1^4 \operatorname{ctg}^4(\alpha_1) \\
 & + 6d_1^4 n_s^2 \operatorname{ctg}^2(\alpha_1) + 2e^2 d_1^2 (n_q^2 + n_a^2) \operatorname{ctg}^4(\alpha_1) \\
 & - 12e^2 d_1^2 n_s^2 \operatorname{ctg}^2(\alpha_1) - 2(n_q^2 + n_a^2)(e^2 + d_1^2)C^2 \operatorname{ctg}^2(\alpha_1) \\
 & - 2(C^2 \operatorname{ctg}^2(\alpha_1)(e^2 n_q^2 + d_1^2) - (e^2 + d_1^2)(C^2 n_s^2 + B^2 \operatorname{ctg}^2(\alpha_1) \\
 & + 4CBn_s \operatorname{ctg}(\alpha_1))) + f_2^9(-4C^3 B(2n_a^2 + 2n_q^2) + 4CB^3 \\
 & - 8n_q^2 e^4 n_s \operatorname{ctg}^3(\alpha_1) + e^4 n_s^3 \operatorname{ctg}(\alpha_1) - 8n_a^2 d_1^4 n_s \operatorname{ctg}^3(\alpha_1) \\
 & + d_1^4 n_s^3 \operatorname{ctg}(\alpha_1) + 8e^2 d_1^2 n_s \operatorname{ctg}^3(\alpha_1)(n_q^2 + n_a^2) - 8e^2 d_1^2 n_s^3 \operatorname{ctg}(\alpha_1) \\
 & - 4(n_q^2 + n_a^2)(e^2 + d_1^2)C \operatorname{ctg}(\alpha_1)(n_s - C + \operatorname{ctg}(\alpha_1)B) \\
 & - 4(C \operatorname{ctg}(\alpha_1)(n_s C + \operatorname{ctg}(\alpha_1)B)(e^2 n_q^2 + d_1^2) - (e^2 + d_1^2) \\
 & \times Bn_s(Cn_s + \operatorname{ctg}(\alpha_1)B)) + f_2^8(C^4(n_a^4 + 4n_q^2 n_a^2 + n_q^4) \\
 & - 6C^2 B^2(2n_a^2 + 2n_q^2) + B^4 + e^4 n_q^4 \operatorname{ctg}^4(\alpha_1) - 12n_q^2 e^4 n_s^2 \\
 & \times \operatorname{ctg}^2(\alpha_1) + n_s^4 e^4 + d_1^4 n_a^4 \operatorname{ctg}^4(\alpha_1) - 12n_a^2 d_1^4 n_s^2 \operatorname{ctg}^2(\alpha_1) \\
 & + n_s^4 d_1^4 - 2e^2 d_1^2 n_a^2 n_q^2 \operatorname{ctg}^4(\alpha_1) + 12e^2 d_1^2 n_s^2 \operatorname{ctg}^2(\alpha_1)(n_q^2 + n_a^2) \\
 & - 2e^2 d_1^2 n_s^4 + 2n_a^2 n_q^2 (e^2 + d_1^2)C^2 \operatorname{ctg}^2(\alpha_1) + 2(n_q^2 + n_a^2) \\
 & \times (C^2 \operatorname{ctg}^2(\alpha_1)(e^2 n_q^2 + d_1^2) - (e^2 + d_1^2)(C^2 n_s^2 + B^2 \operatorname{ctg}^2(\alpha_1) \\
 & + 4CBn_s \operatorname{ctg}(\alpha_1))) - 2((e^2 n_q^2 + d_1^2)(C^2 n_s^2 + B^2 \operatorname{ctg}^2(\alpha_1) \\
 & + 4CBn_s \operatorname{ctg}(\alpha_1)) - (e^2 + d_1^2)B^2 n_s^2) \\
 & + f_2^7(4C^3 B(n_a^4 + 4n_q^2 n_a^2 + n_q^4) - 4CB^3(2n_a^2 + 2n_q^2) \\
 & + 4n_q^4 e^4 n_s \operatorname{ctg}^3(\alpha_1) - 8n_q^2 e^4 n_s^3 \operatorname{ctg}(\alpha_1) + 4n_a^4 d_1^4 n_s \operatorname{ctg}^3(\alpha_1) \\
 & - 8n_a^2 d_1^4 n_s^3 \operatorname{ctg}(\alpha_1) - 8n_a^2 n_q^2 e^2 d_1^2 n_s \operatorname{ctg}^3(\alpha_1) + 8e^2 d_1^2 n_s^3 \\
 & \times \operatorname{ctg}(\alpha_1)(n_q^2 + n_a^2) + 4n_a^2 n_q^2 (e^2 + d_1^2)C \operatorname{ctg}(\alpha_1) \\
 & \times (n_s C + \operatorname{ctg}(\alpha_1)B) + 4(n_q^2 + n_a^2)(C \operatorname{ctg}(\alpha_1) \\
 & \times (n_s C + \operatorname{ctg}(\alpha_1)B)(e^2 n_q^2 + d_1^2) - (e^2 + d_1^2)
 \end{aligned}$$

$$\begin{aligned}
 & \times Bn_s(Cn_s + \operatorname{ctg}(\alpha_1)B)) - 4(e^2 n_q^2 + d_1^2)Bn_s \\
 & - (Cn_s + \operatorname{ctg}(\alpha_1)B)) + f_2^6(-C^4(2n_a^2 n_q^4 + 2n_a^4 n_q^2) \\
 & + 6C^2 B^2(n_a^4 + 4n_q^2 n_a^2 + n_q^4) - B^4(2n_a^2 + 2n_q^2) \\
 & + 6n_q^4 e^4 n_s^2 \operatorname{ctg}^2(\alpha_1) - 2n_q^2 e^4 n_s^4 + 6n_a^4 d_1^4 n_s^2 \operatorname{ctg}^2(\alpha_1) \\
 & - 2n_a^2 d_1^4 n_s^4 - 12e^2 d_1^2 n_a^2 n_q^2 n_s^2 \operatorname{ctg}^2(\alpha_1) + 2e^2 d_1^2 n_s^4 (n_q^2 + n_a^2) \\
 & - 2n_a^2 n_q^2 (C^2 \operatorname{ctg}^2(\alpha_1)(e^2 n_q^2 + d_1^2) - (e^2 + d_1^2) \\
 & \times (C^2 n_s^2 + B^2 \operatorname{ctg}^2(\alpha_1) + 4CBn_s - \operatorname{ctg}(\alpha_1))) \\
 & + 2(n_q^2 + n_a^2)((e^2 n_q^2 + d_1^2)(C^2 n_s^2 + B^2 \operatorname{ctg}^2(\alpha_1) \\
 & + 4CBn_s \operatorname{ctg}(\alpha_1)) - 2B^2 n_s^2 (e^2 n_q^2 + d_1^2)) + f_2^5(-4C^3 \\
 & \times B(2n_a^2 n_q^4 + 2n_a^4 n_q^2) + 4CB^3(n_a^4 + 4n_q^2 n_a^2 + n_q^4) \\
 & + 4n_q^4 e^4 n_s^3 \operatorname{ctg}(\alpha_1) + 4n_a^4 d_1^4 n_s^3 \operatorname{ctg}(\alpha_1) - 8e^2 d_1^2 n_a^2 n_q^2 n_s^3 \operatorname{ctg}(\alpha_1) \\
 & - 4n_a^2 n_q^2 (C \operatorname{ctg}(\alpha_1)(n_s C + \operatorname{ctg}(\alpha_1)B)(e^2 n_q^2 + d_1^2) - (e^2 + d_1^2) \\
 & \times Bn_s(Cn_s + \operatorname{ctg}(\alpha_1)B)) + 4(n_q^2 + n_a^2)(e^2 n_q^2 + d_1^2) \\
 & \times Bn_s(Cn_s + \operatorname{ctg}(\alpha_1)B)) + f_2^4(C^4 n_q^4 n_a^4 - 6C^2 B^2(2n_a^2 n_q^4 \\
 & + 2n_a^4 n_q^2) + B^4(n_a^4 + 4n_q^2 n_a^2 + n_q^4) + n_s^4 n_q^4 e^4 + n_s^4 n_a^4 d_1^4 \\
 & - 2e^2 d_1^2 n_s^4 n_a^2 n_q^2 - 2n_a^2 n_q^2 ((e^2 n_q^2 + d_1^2)(C^2 n_s^2 + B^2 \operatorname{ctg}^2(\alpha_1) \\
 & + 4CBn_s \operatorname{ctg}(\alpha_1)) - (e^2 + d_1^2)B^2 n_s^2) + 2(n_q^2 + n_a^2)B^2 \\
 & \times n_s^2 (e^2 n_q^2 + d_1^2) + f_2^3(4C^3 B n_q^4 n_a^4 - 4CB^3(2n_a^2 n_q^4 + 2n_a^4 n_q^2) \\
 & - 4n_a^2 n_q^2 (e^2 n_q^2 + d_1^2)Bn_s(Cn_s + \operatorname{ctg}(\alpha_1)B)) \\
 & + f_2^2(6C^2 B^2 n_q^4 n_a^4 - B^4(2n_a^2 n_q^4 + 2n_a^4 n_q^2) - 2n_a^2 n_q^2 B^2 n_s^2 \\
 & \times (e^2 n_q^2 + d_1^2)) + f_2 4CB^3 n_q^4 n_a^4 + B^4 n_q^4 n_a^4 = 0. \quad (10)
 \end{aligned}$$

To find the roots we shall use a program written by us in Python. Then, it will be necessary to investigate each root individually for compliance with the experimental data and boundary conditions.

## Conclusion

In contrast to previously used relationships in differential refractometers with Anderson cuvette, equation (10) derived by us will allow (using its roots) performance of a number of analytical studies of the effect of different Anderson cuvette parameters, as well as values of  $n_s$  and  $l$  on the behavior of changes in  $n_m$  when performing measurements in different conditions, as well as determining critical points (maxima and minima) and boundary conditions, where measurement of  $n_m$  is impossible. It is difficult to establish all these conditions experimentally. In previously used relationships derived with different approximations it was extremely difficult to ensure a reliable result.

It is necessary to note that comparison between the calculated shifts  $L$  (Table 1–3), obtained with the use of (8)–(10), and experimental measurements of  $L$  for

check liquids has shown adequacy of the model developed by us, which allows ensuring the possibility to measure  $n_m$  with required error in the set range of refractive index variations. For example, in the range of  $n_m$  variation from 1.4 to 1.5 it is possible to ensure the required mode of measurement using the derived relationships (8)–(10) (by selecting cuvette parameters, refractive index of the reference liquid  $n_s$  and  $l$ ). For example, a change in  $n_m$  by 0.0001 corresponds a shift of laser beam maximum by one photosensitive sensor. Experimental studying of different liquid media (Fig. 4, Table 4) has confirmed it. Previously it was extremely difficult to obtain this result in a differential refractometer.

In addition, the design of differential refractometer developed by us allows reproducing on the laptop screen the shape of laser beam, which is recorded on the linear photodiode array and controlling of, for example, speckles emergence in it due to different reasons. This allows determining the distortions introduced by them and the reasonability of measurement of the laser beam axis position in this case, as well as further prospects of studies of these media by the differential refractometer developed by us, which makes possible the determining of functionality of the instrument to test the state of different media.

Currently, designs of linear photodiode arrays are developed with 2048 sensors and a distance between them of 0.0002 mm. In this case the error of  $L$  measurement will be 0.0001 mm. This will broaden the possibilities of  $n_m$  measurement with higher accuracy.

The results obtained by us allow future development of a verification scheme of the first class for a number of liquid media on the basis of the differential refractometer with Anderson cuvette. For this purpose, it is necessary in laboratory conditions, for example, to measure  $n_m$  in the range from 1.43 to 1.44, to ensure that a change in  $n_m$  by 0.00001 corresponds to a shift of laser beam maximum by one photosensitive sensor. In this case it is possible to get a measurement error of about  $0.2 \cdot 10^{-5}$  with the use of appropriate design of the linear photodiode array, which is close to accuracy characteristics of the state standard.

### Conflict of interest

The authors declare that they have no conflict of interest.

### References

- [1] A.F. Guedes, F.A. Carvalho, C. Moreira, J.B. Nogueira, N.C. Santos. *Nanoscale*, **9** (39), 14897(2017). DOI: 10.1039/c7nr03891g
- [2] V. Antonov, P. Efremov. *Tech. Phys.*, **65** (9), 1446 (2020). DOI: 10.1134/S1063784220090042
- [3] M.S. Mazing, A.Y. Zaitceva, Y.Y. Kislyakov, S.A. Avdyushenko. *Intern. J. Pharmaceutical Research*, **12**, 1974 (2020). DOI: 10.31838/iipr/2020.SP2.355
- [4] V.V. Davydov, N.S. Myazin, S.S. Makeev, V.I. Dudkin. *Tech. Phys.*, **65** (8), 1327 (2020). DOI: 10.1134/S1063784220080058
- [5] A. Bobyl, V. Malyshkin, V. Dolzhenko, A. Grabovets, V. Chernoiyanov. *IOP Confe. Series: Earth and Environmental Science*, **390** (1), 012047 (2019). DOI: 10.1088/1755-1315/390/1/012047
- [6] F. Murzakhonov, G. Mamin, S. Orlinskii, M. Gafurov, V. Komlev. *ACS Omega*, **6** (39), 25338 (2021). DOI: 10.1021/acsomega.1c03238
- [7] E. Verbitskaya, V. Eremin, A. Zabrodskii, N. Egorov, A. Galkin. *J. Instrumentation*, **12** (3), C03036 (2017). DOI: 10.1088/1748-0221/12/03/C03036
- [8] J. Burlakovs, Z. Vincevica-Gaile, M. Krievans, T. Tamm, M. Klavins. *Minerals*, **10** (6), 1 (2020).
- [9] A. Bobyl, I. Kasatkin. *RSC Advances*, **11** (23), 13799 (2021). DOI: 10.1039/d1ra02102h
- [10] V.V. Davydov, N.S. Myazin, V.I. Dudkin. *Tech. Phys.*, **63** (12), 1845 (2018). DOI: 10.1134/S1063784218120046
- [11] A.I. Zhernovoi, A.A. Komlev, S.V. D'yachenko. *Tech. Phys.*, **61** (2), 302 (2016). DOI: 10.1134/S1063784216020274
- [12] M.A. Karabegov, *Measurement Techniques*, **47** (11), 1106 (2004). DOI: 10.1007/s11018-005-0069-1
- [13] N.M. Grebenikova, V.Y. Rud. *J. Physics: Conference Series*, **1410** (1), 012186 (2019). DOI: 10.1088/1742-6596/1410/1/012186
- [14] V.V. Davydov, A.V. Moroz, *Optics and Spectroscopy*, **128** (9), 1415 (2020). DOI: 10.1134/S0030400X20090076
- [15] M.A. Karabegov, *Measurement Techniques*, **50** (6), 619 (2007). DOI: 10.1007/s11018-007-0120-5
- [16] E.V. Rodriguez, A.D. Guzman Chavez. *Opt. Commun.*, **524**, 128765 (2022). DOI: 10.1016/j.optcom.2022.128765
- [17] S.A. Jaywant, H. Singh, K.M. Arif. *Sensors*, **22** (6), 2290 (2022). DOI: 10.3390/s22062290
- [18] M. Condorelli, L. Litti, M. Pulvirenti, M. Meneghetti, G. Compagnini. *Appl. Surfa. Sci.*, **566**, 150701 (2021). DOI: 10.1016/j.apsusc.2021.150701
- [19] M.A. Karabegov, *Measurement Techniques*, **54** (10), 1203 (2012). DOI: 10.1007/s11018-012-9872-7
- [20] K.S. Rashid, L. Tathfif, A.A. Yaseer, M.F. Hassan, R.H. Sagor. *Opt. Express*, **29** (23), 37541 (2021). DOI: 10.1364/OE.442954
- [21] M.A. Karabegov. *Measurement Techniques*, **52** (4), 416 (2009). DOI: 10.1007/s11018-009-9279-2
- [22] P. Gao, X. Zheng, Y. Liu, Z. Wang. *Optik*, **267**, 169682 (2022). DOI: 10.1016/j.ijleo.2022.169682
- [23] A. Kumar, P. Verma, P. Jindal. *J. Opt. Society America B: Opt. Phys.*, **38** (12), F81 (2021). DOI: 10.1364/JOSAB.438367
- [24] V.S. Terent'ev, V.A. Simonov. *Opt. Spectr.*, **129** (11), 1179 (2021). DOI: 10.1134/S0030400X21080191